JOURNAL OF MATERIALS SCIENCE **37** (2002) 3881 – 3892

A Review on the various synthesis routes of TiC reinforced ferrous based composites

K. DAS, T. K. BANDYOPADHYAY, S. DAS
Department of Metallurgical and Materials Engineering, Indian Institute of Technology, Kharagpur 721 302, India
E-mail: Karabi@metal.iitkgp.ernet.in

The major thrust underlying the processing of Fe-based composites has been directed towards improving the wear resistance of steel or cast iron by incorporating some reinforcing phase, e.g., carbides, oxides, etc. The present article provides a review on the various synthesis routes of TiC reinforced Fe-based composites, i.e., powder metallurgy, conventional melting and casting, carbothermic reduction, combustion synthesis, aluminothermic reduction, electron beam radiation, laser surface melting, and plasma spray synthesis, highlighting the advantages and disadvantages associated with the different routes of synthesis.

1. Introduction

Composite materials evolve from the idea of combining two basically dissimilar materials with different physical and mechanical properties to arrive at a product whose final properties are superior to those of the individual components. Composite materials have probably being used since biblical times when man made houses out of mud reinforced with straws. Over the years people have modified the matrix as well as the reinforcement according to their need. The matrix of a composite can be either polymer, metal, or ceramic. Although major applications of composite materials have involved resin-based composites, metal matrix composites (MMC) have also steadily found applications in many areas, especially for high temperature applications. The reinforcement of metals with ceramics causes an increase in strength, stiffness, wear resistance, high temperature strength, and a decrease in weight.

Although most of the work on MMC is centered on light metal alloys to improve upon their strength and stiffness, there is also considerable interest in developing Fe-based MMC's. Iron matrix composites have gained attention essentially for wear resistant applications. Iron and its alloys, as engineering materials, are yet to be displaced from the top slot by polymers, ceramics, or other metals in terms of volume of consumption; thus it becomes imperative to further improve their properties. Achieving the same by ceramic particle reinforcement is possible and has been proved [1–3]. The common ceramic materials used for reinforcing Fe matrices are Al_2O_3, ZrO_2, TiN_2, Si_3N_4, TiC, B_4C, VC etc. Among them TiC has proved its suitability in Fe or Fe base alloys due to its high hardness, good wettability, low density, and its chemical stability with Fe-based matrices [4, 5]. However, it is the economy of processing the composite that will decide if it is able to compete against the wide range of steels already available in the market. As material designers are in constant search for noble and economical synthesis route, the various routes of synthesis of TiC reinforced Fe-based composites have been evolving over the years gradually. The present article provides a review on various synthesis routes of Fe-TiC composites, with emphasis on advantages and disadvantages associated with different methods.

2. Routes of synthesis

Various routes that have been used in synthesizing Fe-TiC composites are

(i) Powder metallurgy route
(ii) Conventional melting and casting route
(iii) Carbothermic reduction route
(iv) Combustion synthesis route
(v) Aluminothermic reduction route
(vii) Electron beam radiation/laser surface melting/ plasma spray synthesis route

2.1. Powder metallurgy route

Powder metallurgy route has been used widely to produce TiC reinforced Fe-based composites because [6, 7]

(i) These materials are difficult to fabricate by the conventional liquid processing route owing to the high processing temperature involved.
(ii) It offers the possibility of using a wide range of reinforcement volume fraction and size.
(iii) It also ensures a homogeneous distribution of reinforcements in the matrix material.
(iv) A high dislocation density, a small subgrain size and limited recrystallization can be obtained through a PM route, resulting in superior mechanical properties.

TABLE I List of some commercially available Fe-TiC composites

Trade name	Composite	Manufacturer	Processing method
FERROTiC	TiC/hardenable tool, stainless, or alloy steel	Alloy Technology Inc. (USA)	Vacuum sintering at 1500°C
TiCALLOY	TiC/heat treatable alloy steel matrix	Seilstorfer (Germany)	Hot isostatic pressing
FERROTITANIT	TiC/high alloy steel	Thyssen (Germany)	

TABLE II Fe-TiC composites developed by M/s. Alloy Technology Inc., USA

Grade	Carbide (vol%)	Matrix alloy type	Remarks
CM	45	High chrome tool steel	Good temper resistance, wear parts or general purpose tooling and heavy forming upto 600°C
C	45	Medium alloy steel	Tools, dies and wear parts. Excellent dampening in annealed condition
SK	40	Hot work tool steel	Good thermal shock and impact resistance, hot work applications, cold heading dies and hammers
CS-40	45	Martensitic stainless	High hardness with corrosion resistance of 400 series stainless steels
J	40	High speed steel	Good resistance to high temperature for elevated temperature tooling upto 730°C
S-45	45	Austenite stainless steel	Excellent corrosion resistance of 300 series stainless steels

Iron-based TiC reinforced composites, which are commercially available (Table I) [8] are produced through a powder metallurgy route. Table II gives the details of the different types of Fe-based composites produced by Alloy Technology Inc. (USA) [9]. Among the powder metallurgy routes, hot isostatic pressing (HIPing) is used more frequently, since it produces more homogeneous material compared to its corresponding cast grades, which in turn improves the fracture properties [2, 10]. It can also produce a near net shape product, which is otherwise difficult to produce due to the problem that arises during machining and trimming of a very hard material. It can also produce fully densified material.

Pagounis, Talvitie and Lindroos [1, 2, 6] worked extensively on TiC reinforced white Fe matrix/tool steel matrix composites produced by hot isostatic pressing. In order to assess the influence of the reinforcement volume fraction on the microstructure and abrasion resistance of white Fe matrix composites, high-Cr white Fe powder was mixed thoroughly with 10, 20 and 30 vol% stoichiometric TiC powder, and then HIP'd under the condition of 1180°C, 100 MPa pressure, and 3 hour holding time. The HIP'd materials were then subjected to austenitization followed by air cooling and tempering. The effect of reinforcement particle size on wear resistance was also studied by varying the TiC powder sizes (fine TiC particles having a size distribution of 5.6 to 22.5 μm and coarse TiC particles having a size distribution of 50 to 100 μm). It was found by the authors [1] that the wear resistance increased with the increase in reinforcement volume fraction until the spallation of the second phase occurred and also, that the composites reinforced with fine particles were more wear resistant compared to the composite reinforced with coarse particles (Fig. 1). The authors concluded that the microstructures of the unreinforced and reinforced materials were different in spite of the same heat treatment procedure. This was due to the presence of a tensile stress into the matrix of the composite material caused by the different coefficients of thermal expansion (CTE) of matrix and reinforcement. This tensile stress was responsible for increased martensitic transformation and hence a decreased amount of retained austenite and this in turn

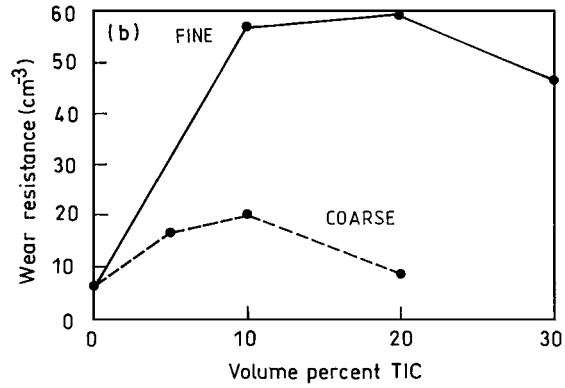

Figure 1 Wear resistance vs. TiC volume fraction for high-Cr white iron (Fe-26 wt% Cr-2 wt%C)/TiC composites austenized at 1160°C [1].

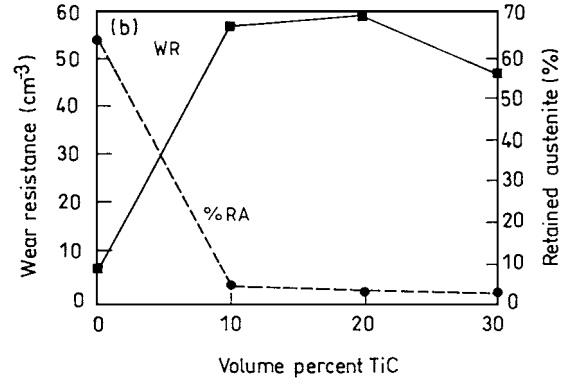

Figure 2 Wear resistance (WR) and the amount of retained austenite (%RA) vs. fine TiC volume fraction, for high-Cr white iron/TiC composite austenized at 1160°C [1].

increased the wear resistance of the material. Fig. 2 depicts how the amount of retained austenite and the wear resistance vary with the volume fraction of fine TiC particles.

In order to assess the effect of matrix structure on the abrasion wear resistance and toughness of white Fe matrix composite, white Fe powder (60 percent of the particles are <75 μm and 40 percent are 75 to 150 μm) was mixed thoroughly with 10 vol% TiC particle (particles having 5.6 to 22.5 μm size) and then HIP'd. Composites were subjected to nine different heat treatment procedures. The authors concluded that parameters like

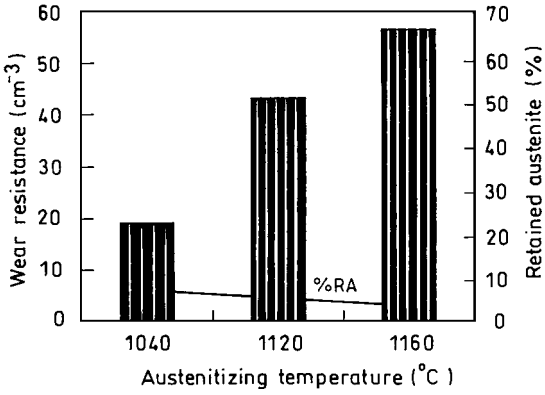

Figure 3 Wear resistance (in bars) and retained austenite content (%RA, in line) vs. austenitizing temperature, for the high-Cr white iron/TiC composite [2].

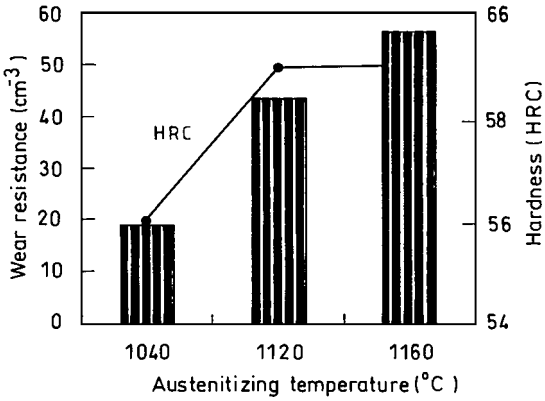

Figure 4 Wear resistance (in bars) and hardness (in line) of the high-Cr white iron/TiC composite vs. austenitizing temperature [2].

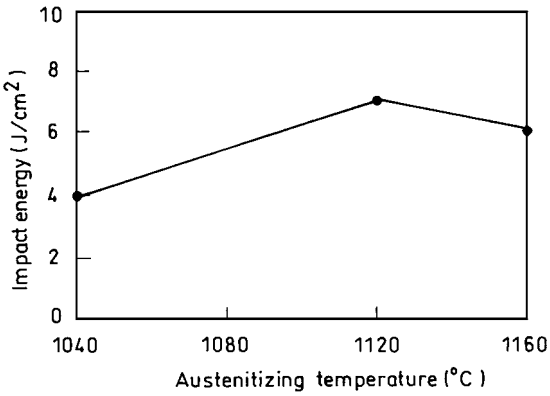

Figure 5 Impact energy of the high-Cr white iron/TiC composite vs. austenitizing temperature [2].

austenitizing temperature of the matrix had a critical role in determining the final performance of the composite, i.e., wear resistance, hardness, and toughness (Figs 3–5).

In a subsequent paper Pagounis *et al.* [6] described the microstructure and mechanical properties of hot-worked tool steel matrix composites produced by hot isostatic pressing. Here, hot-worked tool steel powder was mixed with three different types of carbides, TiC, Cr_3C_2, or VC. Three different composites, i.e., hot-worked tool steel and TiC or Cr_3C_2 or VC were HIP'd at 1100°C temperature, 100 Mpa pressure, and 3 hour holding time. The authors found that (i) there was phenomenal improvement of wear resistance and a much greater hardness than the unreinforced alloy (ii) there was a uniform distribution of reinforcing phase in fully densified material, and (iii) there was no significant reaction between alloy matrix and ceramic particles. However, the toughness of the composite was reduced.

Bolton and Gant [11] studied the microstructural development and sintering kinetics of high-speed steel based composites reinforced with either TiC or NbC. The composites were made though a conventional sintering route. It was concluded by the authors that the relative volume fraction, composition and type of primary carbides present in the high speed steel were altered due to the presence of TiC or NbC in the composites.

Production of composite via a powder metallurgy route has its limitations. Mixing of matrix powder and reinforcing particle must be thorough in order to achieve uniform dispersion of the reinforcing phase. The Sintering cycle and environment must be chosen critically to obtain components with near theoretical density. There is also difficulty in machining or trimming of sintered parts because of high hardness of the materials, and the mold designs must be simple in order to prevent density differences during compacting and sintering [12]. One then looks to the other common route, the melting and casting route, for synthesizing composite materials.

2.2. Conventional melting and casting route

Attempts have been made to produce Fe-based composites through alternative cost effective process such as *in situ* production of Fe-TiC composites by reaction in liquid Fe alloys [3, 8, 13–18]. Interest in the development of the *in situ* technique to produce particulate metal matrix composites has its roots behind the following reasons [8]:

1. The process enables the formation of clean interfaces, i.e., free from adsorbed gases, oxides or other detrimental surface reactions. This in turn tends to make the matrix-filler interface bond strong.
2. The process of generation of the filler phase *in situ* excludes the manufacture and the handling of the phase separately; thereby reducing the unit steps in the process.
3. Near net shape final components can be produced by direct casting.

Terry and Chinyamakobvu [8] produced Fe-TiC composite by adding C in the form of coal to molten Fe-Ti alloy in an induction furnace. The melt was maintained at 1550°C for 20 minutes to complete the reaction. The composite was also produced by an addition of Ti filings to a levitated drop of 3 wt% carbon cast iron. The reaction at 1600°C for 80 seconds virtually completed the conversion of Ti to TiC. The microstructure of the composites produced by both methods showed a uniform distribution of discrete TiC particles.

The degree of dispersion that can be achieved in liquid matrices is known to depend on various process parameters namely temperature, liquid matrix composition, composition and surface properties of dispersoid, and ambient atmospheric condition [13]. Though

wettability is an important criterion, one cannot assess the degree of dispersion by knowing the wettability alone. Terry *et al*. [13] developed a dispersion test for TiC dispersed Fe composite. The test relies on electromagnetic levitation of a molten metal drop with the dispersoid phase where the effects of parameters like melt composition, gas atmosphere, surface properties of dispersoid and temperature on degree of dispersion can be studied easily. The dispersion test provides qualitative assessment of dispersion as the levitated metal-dispersoid phase droplet is quenched and examined by optical/electron microscope and phases identified by X-ray diffraction. There are several advantages of such a levitation test: (i) the use of a ceramic crucible is eliminated and therefore, crucible material contamination is avoided, (ii) well mixed heterogeneous melts are obtained which can indicate the wetting of the solid component achieved as a result of vigorous stirring, (iii) gas surrounding the melt can be changed and its effects can be studied, and (iv) a quick heating and attainment of equilibrium provide the basis for a rapid test procedure. However, the limitation of the test lies in its inability to assess the segregation behaviour of the dispersiod as the quantity of the charge is quite small.

Raghunath *et al*. [14] prepared Fe-TiC composites in a MgO lined induction furnace with a blanket of N_2 gas over the melt. The ductile iron was melted in the furnace and upon reaching the temperature of 1450°C, ferro titanium was added. The composites containing up to 10 vol% TiC was statically cast. However, the composites containing large volume fraction of TiC could not be poured. Therefore, it was squeezed under a pressure of 1000 psi and allowed to solidify in the crucible within the furnace followed by remelting and solidification under vacuum (10^{-6} torr) in a resistance furnace. The microstructure of the composite showed uniform distribution of spheruletic carbides.

Skolianos *et al*. [15] prepared Fe-TiC composites in a high frequency induction furnace by melting pieces of stainless steel and then adding the appropriate amounts of Ti and graphite under an argon atmosphere. The cooling rate was varied by casting the composite in a graphite or a cast iron mould. The authors concluded that (i) the specific wear rate decreased with increasing volume fraction of carbide and decreasing particle size and spacing, and (ii) for a given volume fraction of carbide and carbide particle size (a) the wear rate increased with a softer matrix and (b) the friction coefficient decreased with the microhardness of the matrix.

TiC reinforced Fe-based (Fe-Mn-Ti-C) composites were made by melting the alloy at 1873 K in an induction furnace under an inert atmosphere followed by gas atomisation with high purity argon by Popov *et al*. [16]. The microstructure of the materials showed a uniform distribution of very fine TiC particles (0.3–0.5 μm) in an austenetic matrix.

The Fe-TiC composites were made by Kattamis *et al*. [3] by (i) precipitation of TiC from a Fe-Ti-C melt and (ii) dispersion of TiC particles in an Fe-C melt by vigorous electromagnetic mixing. In the first process, cast iron was melted in an induction furnace under argon and then appropriate amounts of Ti and Fe were added to get different volume fractions of TiC. Melts were undercooled and nucleated at about 10°C below the TiC liquidus followed by either rapid quenching (resulting martensitic matrix), or argon cooling/slow cooling (resulting pearlitic matrix). In the second process, iron, low carbon steel, or cast iron was melted in an induction furnace under an argon atmosphere and then the TiC particles were mixed through an electromagnetically induced stirring. The melt was held at different temperatures (1200°C to 1700°C) for various times (0 to 250 s) followed by slow cooling in the furnace, argon cooling, or water quenching. The authors concluded that the microstructure of the composite obtained by precipitation of TiC from Fe-Ti-C melt could be altered by controlling the melt composition, uniformity, and cooling rate, whereas the microstructure of the composite produced by dispersing TiC particles in steel or cast iron melt could be controlled by controlling the original melt composition, volume fraction and size of TiC added, mixing temperature and time, and cooling rate. It was also concluded by the authors that the specific wear rate and the friction coefficient between a diamond stylus and polished specimen surface decreased with the increase of TiC volume fraction and with the decrease of carbide particle size and spacing.

It is quite clear from the above discussion that all the composites were produced either by adding C to Fe-Ti alloy or Ti to Fe-C alloy and the proportion of each element was adjusted to get the desired volume fraction of TiC as well as the matrix composition [3, 8, 14, 15]. However, Katamis and Suganuma [3] also produced the Fe-TiC composites by mixing TiC powder in steel/cast iron melt. The composites produced by all the above-mentioned authors were reinforced with 10–15 μm size TiC particles. It has been well established that the wear resistance of a Fe-TiC composite increases with the decrease in particle size. Popov *et al*. [16] was able to get 0.3 to 0.5 μm size TiC particle by gas atomization of the melt.

However, the conventional melting and casting route has some limitations. A high processing temperature is required to fabricate Fe-based composites by a conventional liquid processing route. Also, the maximum Ti and C contents in the melt should be restricted to 8–10 wt% and 3–4 wt%, respectively to obtain optimum fluidity [12]. Therefore, smelting route is only applicable for the preparation of ferrous composites with a low volume fraction of TiC. The other problem that may arise is the non-uniform distribution of the carbide particles. One way to avoid this problem is to increase the solubility of TiC in the alloy resulting in a uniform distribution of TiC particles. Popov *et al*. [16] did some thermodynamic calculations to show that an addition of Mn in Fe-C alloy increased the solubility of TiC in the alloy resulting in a uniform distribution of TiC particles.

2.3. Carbothermic reduction route

The slope of the $C(s) + O_2(g) = 2CO(g)$ line in the Ellingham diagram is reverse to those of the other oxides [19]. Therefore, the C-CO line intersects many oxide lines. It is thus possible to reduce many oxides (i.e., Cu_2O, PbO, Fe_3O_4, ZnO, MnO, etc.) by C above

the temperature at which the C-CO line intersects their oxide lines. Carbon being very cheap, in the form of either charcoal or coke, is used for commercial production of these metals from their oxides. These reduction processes have to be carried out at high temperatures, and hence these are known as carbothermic reduction process. Some researchers produced the Fe-TiC composite by carbothermic reduction of ilmenite or rutile [8, 12]. The feasibility of various reactions and temperatures required for smelting of ilmenite by C can be readily ascertained by the knowledge of thermodynamics [20]. Two most important reactions that can be considered are as follows:

$$FeTiO_3\ (s) + 3C\ (s) = Ti\ (s) + Fe(s) + 3CO\ (g) \quad (1)$$
$$\Delta G^{o}_{T} = 202,968.3 - 117.56T\ \text{Cal}$$

Hence, $\Delta G^{o}_{T} = 0$ at $T = 1726.5$ K

$$FeTiO_3\ (s) + 4C\ (s) = Fe(s) + TiC\ (s) + 3CO\ (g) \quad (2)$$
$$\Delta G^{o}_{T} = 158{,}368.3 - 114.4T\ \text{Cal}$$

Hence, $\Delta G^{o}_{T} = 0$ at $T = 1384.3$ K

It may be noted that TiC formation requires a lower temperature compared to that for the formation of metallic Ti. Hence, the reaction product of carbothermic reduction of ilmenite would contain TiC in an Fe matrix.

Terry *et al*. [21] tried direct carbothermic reduction of ilmenite ($FeTiO_3$) or rutile (TiO_2) to produce small quantities of composite. The following reactions were considered by the authors [21]:

$$XFe + FeTiO_3 + 4C = (x+1)\,Fe + TiC + CO \quad \text{(for ilmenite)}$$

$$XFe + TiO_2 + 3C = x\,Fe + TiC + 2CO \quad \text{(for rutile)}$$

In order to obtain a required Fe/TiC ratio in the composite, an excess amount 'x' of iron powder was added. In this process pellets consisting of Fe powder (C saturated), rutile or ilmenite, collie coal mixture in various proportions was heated in a tube furnace in the temperature range of 1300°C to 1600°C under a flowing argon atmosphere. The process produced Ti (O,C) rather than TiC as the reinforcement phase and it was attributed to a lower reduction temperature. Excellent dispersions of Ti (O,C) were obtained above 1450°C.

Galgali *et al*. [12] worked extensively on the preparation of TiC rich Fe-TiC master alloys and TiC reinforced cast iron composites by carbothermic reduction of ilmenite in a bed of steel scrap using a plasma reactor. As it was not possible to obtain TiC reinforced steel based composites by carbothermic reduction of ilmenite in a bed of steel scrap using a plasma reactor in a graphite crucible, steel composites were prepared by dissolving TiC rich Fe-TiC master alloy in plain carbon or alloy steel melts in an induction furnace.

Another work in similar lines was carried out by Chen *et al*. [22] and it was found that an improvement in the efficiency of the above process to obtain composite could be achieved by high-energy ball milling of the reaction mixture. It was shown by the authors [22] that even at 1000°C, Fe-TiC composite could be produced from a ball milled mixture of ilmenite and graphite.

The advantage of producing Fe-based composites through carbothermic reduction of ilmenite is the reduction of a number of steps and thereby the cost of production. On the other hand, the carbothermic reduction leading to the formation of TiC in Fe matrix is endothermic though spontaneous above 1384.3 K, as can be seen from Equation 2. Hence, the system should have enough heat to supply for the reaction besides melting the charge. In any process route energy being a costly input, it makes sense to minimize this variable. An alternative energy efficient route to produce Fe-TiC composite is discussed in the following section.

2.4. Combustion synthesis route

The combustion synthesis, reaction synthesis, or self-propagating high temperature synthesis (SHS) can be defined as a process where the heat liberated due to exothermic reaction is adequate to sustain the reaction by the rapid propagation of a combustion front without further addition of energy. In the early days, their applications were limited to pyrotechnics and rocket fuel [23]. However, in recent years this method is being utilized to produce a wide variety of ceramics, ceramic-composites, and intermetallic compounds. Compared to conventional ceramic processing, the most obvious advantages of combustion synthesis are primarily [24]: (1) the generation of a high reaction temperature which can volatilize the low boiling point impurities and therefore, result in high purity products, (2) the simple exothermic nature of the SHS reaction avoids the need for expensive processing facilities and equipment, (3) the short exothermic reaction time results in low operating and processing costs, (4) the high thermal gradients and rapid cooling rates can give rise to new non-equilibrium or metastable phases, (5) inorganic materials can be synthesized and consolidated into a final product in one step by utilizing the chemical energy of the reactants.

A schematic representation of a temperature-time plot for a combustion synthesis reaction is given in Fig. 6. In the figure the ignition temperature, T_{ig}, is that temperature where the exothermic reaction is initiated and the heat generation due to exothermic reaction

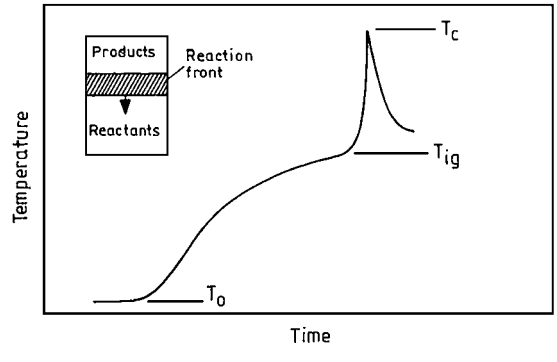

Figure 6 Schematic representation of the time-temperature curve during an SHS reaction [24].

is manifested by the maximum or combustion temperature, T_c.

The combustion synthesis reaction can be conducted in two modes: (1) self-propagating mode, often referred to as SHS, and (2) simultaneous combustion mode often referred to as thermal explosion. In the self-propagating mode, a small part of the reactant is ignited at a high temperature creating a combustion wave, which propagates through the entire sample. In contrast, the simultaneous combustion mode occurs when the reaction takes place simultaneously throughout the reactant mixture once the entire sample has been heated to the ignition temperature. Typical experimental set-ups used for thermal explosion mode and normal SHS mode are shown in Fig. 7a and b [25]. The difference between the combustion and thermal explosion mode was indicated in a SHS diagram (Fig. 8) by Sato and Munir [26]. In this diagram the starting temperature is plotted against degree of dilution. The degree of dilution with respect to Fe-TiC system is determined by the Fe content.

The combustion synthesis of the Ti-C system has been studied extensively [27–38]. However, the present article deals with the synthesis of the Fe-TiC composite. Therefore, we will be discussing those studies, which involve the synthesis of Fe-TiC composite by combustion synthesis mode. Saidi *et al*. [39] used the thermal explosion mode to produce Fe-TiC composite. Carbon black and Ti powders were mixed at an equiatomic ratio.

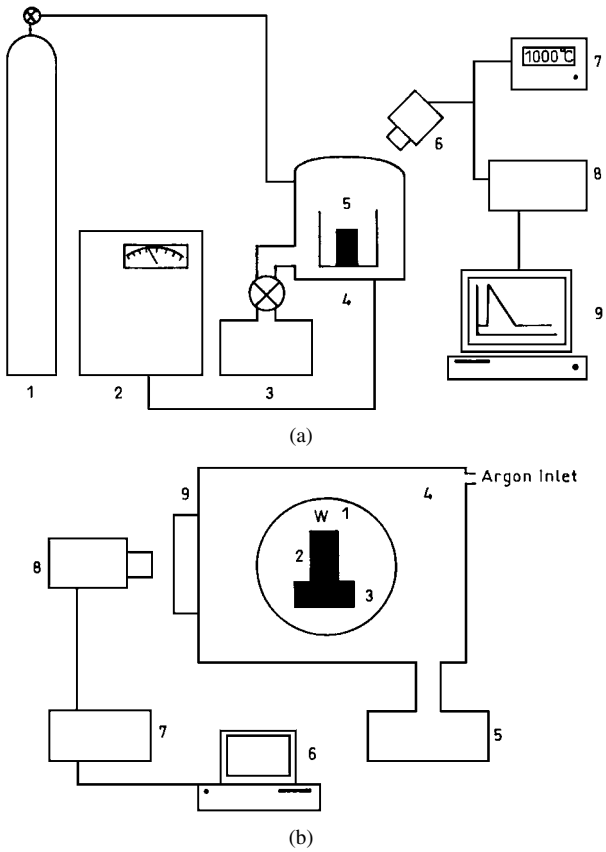

Figure 7 (a). Apparatus used for Thermal Explosion (TE) experiments. (1) argon supply, (2) power supply, (3) vacuum pump, (4) furnace chamber, (5) sample, (6) pyrometer, (7) temperature display, (8) data acquisition system, (9) PC [25]. (b). Apparatus used for normal SHS experiments. (1) tungsten filament, (2) sample, (3) graphite stage, (4) glove box, (5) vacuum pump, (6) PC, (7) data acquisition system, (8) pyrometer, (9) quartz window [25].

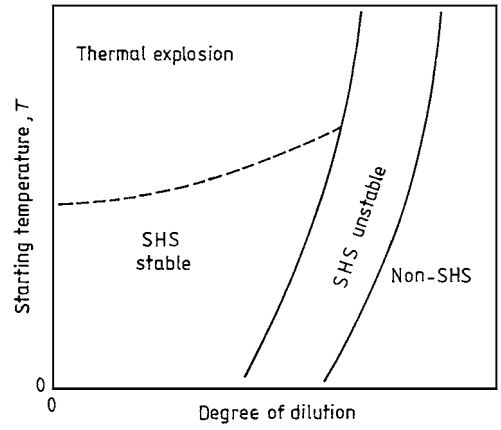

Figure 8 Schematic representation of an SHS diagram [26].

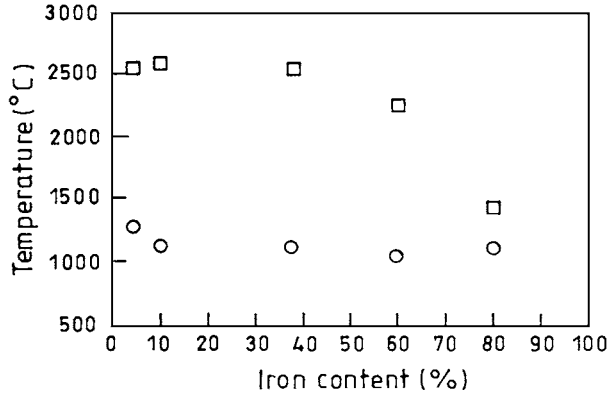

Figure 9 Plots of ignition temperature (○) and combustion temperature (□) as a function of Fe content [39].

Then, the Fe powder was added to obtain products with Fe compositions ranging from 2.7% to 85%. The powder mixture was compacted in a ceramic die rather than in a steel die to avoid segregation of Fe due to its magnetic effect. The precompacted samples were heated to the ignition temperature under an argon atmosphere in an induction furnace. The authors suggested that Ti and Fe powders reacted in the solid state to produce $FeTi_2$, which was a eutectic compound having a melting point of 1085°C. At the ignition temperature, which was very close to the melting point of Fe-Ti alloy, C dissolved in the molten droplets of $FeTi_2$ and subsequent formation of TiC released enough heat to initiate a self-sustaining reaction. The authors also found that an increase in the amount of Fe led to a decrease in the combustion temperature, as more of the exothermic heat was absorbed (Fig. 9). The ignition temperature decreased initially with the addition of Fe and then it reached a steady state temperature with increasing Fe content near the eutectic temperature in the Fe-Ti phase diagram. In a subsequent paper Capaldi, Saidi, and Wood [25] studied the combustion synthesis of Fe-TiC by both thermal explosion and normal SHS mode. It was found that the morphology of the products obtained was similar in both reaction modes. The mechanism of formation of Fe-TiC as suggested by Capaldi *et al*. [25] was similar to that of as suggested by Saidi *et al*. [39] and Choi *et al*. [40]. Capaldi *et al*. [25] also measured the activation energy to support the suggested mechanism of formation of Fe-TiC.

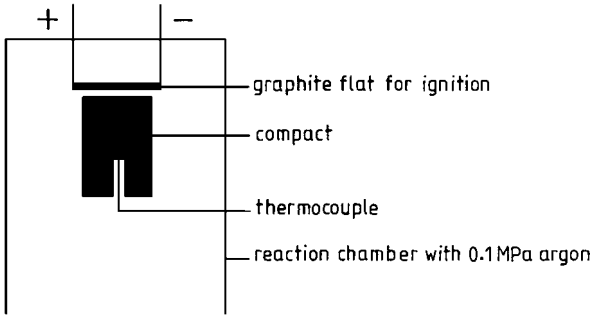

Figure 10 Schematic diagram of combustion temperature measurement [41].

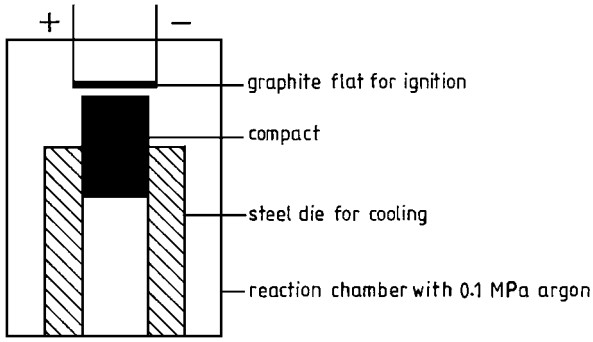

Figure 11 Schematic diagram of the combustion front quenching test [41].

Fan *et al.* [41] conducted the following experiment in order to evaluate the microstructural evolution of TiC-Fe by the combustion synthesis. Iron powders (<45 μm diameter) of amount 30 wt% were incorporated into a mixture of Ti powders (135-154 μm) and carbon black (0.033–0.079 μm diameter) with an equiatomic ratio and they were mixed thoroughly. A compact (14 mm diameter and 18 mm length) with a relative density of about 60% was made from the powder mixture. In order to measure the combustion temperature, a small hole was drilled at the bottom of the compact, and a thermocouple pair of W-3% Re and W-25% Re was inserted into the hole and linked up with an X-Y recorder by means of which a temperature-time curve could be recorded. The compact was ignited in a reaction chamber with an incandescent graphite flat placed 2 mm above the top surface of the compact at a pressure of 0.1 MPa of argon at an initial temperature of 298 K, and the temperature-time curve was recorded as the combustion wave self propagated through the compact (Fig. 10). The combustion temperature was determined by the temperature maxima of the curve. The authors also conducted a combustion front quenching test by pushing out a part of the green compact from the die. The compact was ignited at the top surface with an incandescent graphite flat (Fig. 11). The combustion wave self propagated in the compact, but got self quenched before the front reached the bottom of the compact because of the cooling effect of the steel die. Authors [41] suggested the followings:

(a) The combustion reaction in Ti particles mainly took place in the solid state. The conclusion was based on two observations: (i) SEM micrograph showed that the shape and size of the reacting Ti particle were not different from those of the initial Ti particles, (ii) The measured combustion temperature is 1903 K, which is lower than the melting point of Ti (1945 K).

(b) The reaction started at the surface of the Ti particle and then proceeded by the solid-state diffusion of C and Fe atoms into the Ti particles forming TiC together with a binder phase consisting of Fe and Ti.

(c) The TiC particles appeared as isolated spherical particles surrounded by the binder phase, and were not agglomerated or angular. This was quite different from the TiC particles that formed in the binary Ti-C system.

In the binary system the combustion product consisted of only TiC particles of angular shape. This was well known; because of the requirement of a driving force for diffusion only a single phase was able to exist in a binary reaction-diffusion layer of a binary system, whilst two phases were able to exist simultaneously in a ternary-reaction-diffusion layer of a ternary system [42]. Therefore, in the Ti-C-Fe system, the TiC particles formed in the ternary-reaction-diffusion layer together with the binder phase separating the TiC particles had to be isolated and spherical ones. Fig. 12A and B shows

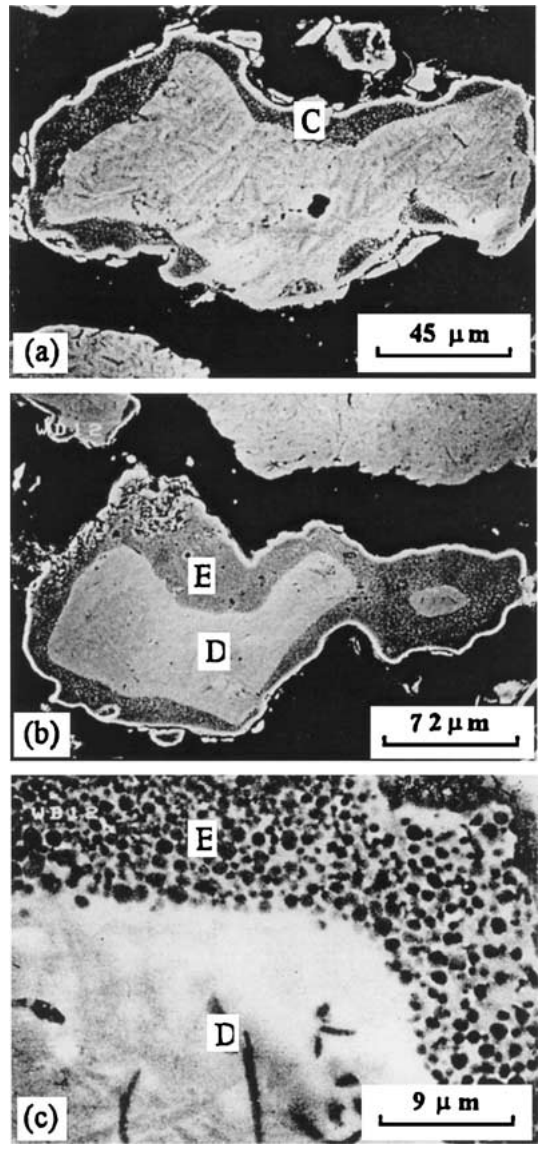

Figure 12A Scanning electron micrographs of reacting Ti particles: (a) starting from the surface layer, (b) propagating towards the center, and (c) the reaction product [41].

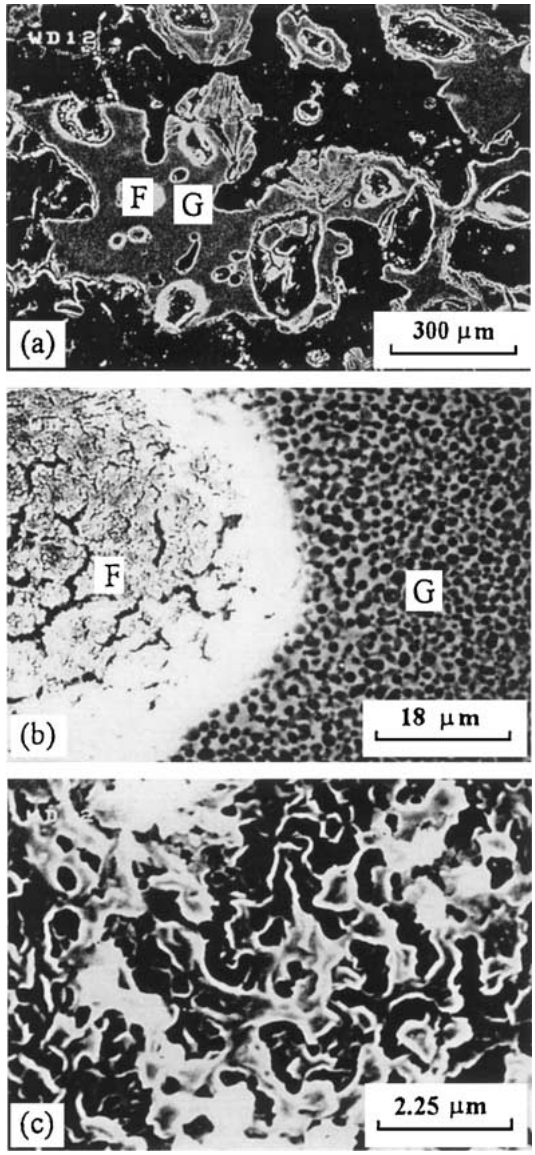

Figure 12B Scanning electron micrographs of the fusion and flow of reacted Ti particles: (a) the macrostructure, (b) the microstructure of interface 'F'/'G', and (c) enlargement of region 'F' [41].

the microstructure of the reacting Ti particle and reacted Ti particle. The presence of the residual phase, FeTi (Fig. 12B), was due to the use of the coarse Ti powder leading to a low combustion temperature and a long diffusion distance.

From the above discussion it is quite clear that the combustion synthesis of the Ti-C system has been studied quite extensively. Later, Fe is added to Ti-C system to study the effect of degree of dilution on TiC combustion synthesis and this gives us some information regarding the synthesis of TiC-Fe composite rather than Fe-TiC composite. It can be concluded from the literature [25, 39, 40] that near the ignition temperature Fe and Ti form a low melting point alloy and then C diffuses to form spherical TiC particles separated by a binder phase consisting of Fe and Ti. However, Fan *et al*. [41] suggested that in the Fe-TiC system the reaction took place mostly in the solid state.

2.5. Thermit reduction route

Thermit reaction can also be used as a means to synthesize composite materials. The type of reaction involving reduction of a metallic or a non-metallic oxide with a metal to form a more stable oxide and the corresponding metals or non-metals of the reactant oxide is called the thermit reaction [43]. This form of oxidation-reduction reaction can be written as

$$M + AO = MO + A + \Delta H$$

Where M is a metal, A is either a metal or a non-metal, MO and AO are their corresponding oxides and ΔH is the heat generated by the reaction. Because of the large exothermic heat, a thermit reaction can generally be initiated locally and can become self-sustaining, a factor which makes their use extremely energy efficient. The Ellingham diagram shows that some metals such as Al, Zr, Mg, Ca, etc. form very stable oxides. Therefore, these metals can be used to reduce many oxides such as Cu_2O, Fe_2O_3, SiO_2, TiO_2, etc. The most commonly used reductant is Al due to the following reasons:

i) Although Mg and Ca form two of the most stable oxides, their reducing tendency decreases more sharply at elevated temperatures. Moreover, both Ca and Mg are more volatile having normal boiling point at 1757 and 1363 K, respectively and thus are less desirable for certain applications because of high reaction pressure and vaporization losses [43].

ii) Between Al and Zr, Al is used more commonly because of its availability, although Al and Zr have a comparable reducing tendency.

iii) From the cost standpoint, Al is cheaper than Mg, Ca, or Zr.

iv) The fact that many thermit reactions yield a molten product that consists of a heavier metallic phase and a lighter oxide phase, which can be separated by gravity, makes these reactions potentially useful in many metallurgical applications [43]. The melting point of Al_2O_3 ($T_{mp,Al2O3} = 2051°C$) is lower than those of CaO ($T_{mp,CaO} = 2580°C$) and MgO ($T_{mp,MgO} = 2800°C$). This lower melting point of Al_2O_3 facilitates phase separation.

Thermit reactions that use aluminum as the reducing agent are commonly known as aluminothermic reduction process. This type of reaction is highly exothermic in nature and if the reaction is initiated locally it can become self-sustaining. Although, the aluminothermic reduction can be classified as a class of SHS reaction, the advantage of aluminothermic reduction over SHS is that the starting material for aluminothermic reduction are naturally occuring oxides which are less expensive and more readily available than elemental reactant powders which are the starting materials for conventional SHS process [43], as described in Section 2.4. Aluminothermic reduction has been used to produce a wide variety of composite materials over the last three decades and a partial list of these is given in Table III [43]. However, the authors of the present article could not locate any literature, which deals with the synthesis of Fe-TiC composite by aluminothermic reduction.

The authors of the present article have used the aluminothermic reduction process to produce Fe-TiC composite from an industrial waste [44]. The waste material is called siliceous sand and it is obtained from an Al

TABLE III Reactions for synthesizing composite materials

	Reactions
1.	$Cr_2O_3 + 2Al = 2Cr + Al_2O_3$
2.	$2ZrO_2 + 2SiO_2 + 16/3\ Al = 8/3\ Al_2O_3 + ZrSi_2 + Zr$
3.	$TiO_2 + B_2O_3 + 10/3Al = TiB_2 + 5/3Al_2O_3$
4.	$TiO_2 + 4/3\ Al + C = TiC + 2/3\ Al_2O_3$
5.	$3Fe_3O_4 + 8Al = 9Fe + 4Al_2O_3$
6.	$SiO_2 + 4/3Al + C = SiC + 2/3Al_2O_3$
7.	$2B_2O_3 + 4Al + C = B_4C + 2Al_2O_3$
8.	$2MoO_3 + 4Al + C = Mo_2C + 2Al_2O_3$
9.	$3TiO_2 + 4Al + 3/2C + 3/4N_2 = 3Ti(C_{0.5}N_{0.5}) + 2Al_2O_3$
10.	$3TiO_2 + 4Al + 1.5NaCN = 3TiC_{0.5}N_{0.5} + 2Al_2O_3 + 1.5Na$
11.	$6Mg + 2B_2O_3 + C = 6MgO + B_4C$
12.	$SiO_2 + Al = Si + Al_2O_3 + N_2 +$ heat = β-sialon, 15R-sialon, Al_2O_3, AlN
13.	$Al + SiO_2 + C + N_2 =$ SiC, AlN, AlON, Al_2O_3

TABLE IV Composition of siliceous sand

Composition	Fe_2O_3	Al_2O_3	TiO_2	Na_2O	SiO_2
Wt%	73.1	6.26	8.63	2.51	3.84

extraction plant. A typical sand composition is shown in Table IV. The other impurities like NiO, Cr_2O_3, and V_2O_5make up the balance. The sand is rich in Fe_2O_3 and also contains a substantial amount of TiO_2. The Fe-TiC composite is produced by aluminothermic reduction of siliceous sand in presence of C. The charge needed to synthesize the composite consists of siliceous sand, Al powder, and C in the form of cast iron and/or graphite. Sometimes TiO_2 was added externally to adjust the volume fraction of TiC. The charge was preheated in a pit furnace upto 775°C in a clay graphite crucible. The crucibles were coated with zircon paint to prevent C pick up. The crucible was removed out of the furnace when the requisite temperature of 775°C is reached and then the reaction was triggered by adding Mg turnings. The heat generated due to the aluminothermic reduction was high enough to melt the charge completely and uniformly. A bottom pouring arrangement was made so that the liquid metal can be poured directly into a mould by opening the plug at the bottom of the crucible. A flow chart depicting the synthesis of Fe-TiC composite from siliceous sand is shown in Fig. 13.

The important reactions leading to Fe-TiC composite can be written as

$$3TiO_2 + 4Al + 3C = 3TiC + 2Al_2O_3 \quad (1)$$

$$Fe_2O_3 + 2Al = Al_2O_3 + 2Fe \quad (2)$$

$$SiO_2 + 2Al = Si + Al_2O_3 \quad (3)$$

The composite thus obtained has Fe matrix with some Al, Si, and C dissolved in it and TiC as the reinforcement. A typical microstructure is shown in Fig. 14. The hardness of the as cast composite varied between Rc 48 to Rc 56. The variation in the hardness is mainly due to the variation of volume fraction of TiC and microstructure of the matrix material. The Fe-TiC composite thus obtained has shown very promising wear resistance properties. The wear resistance property of the composite is even better than some of the common tool materials such as M2 grade tool steel. A plot comparing the wear behavior of Fe-TiC composite and tool steel is shown in Fig. 15.

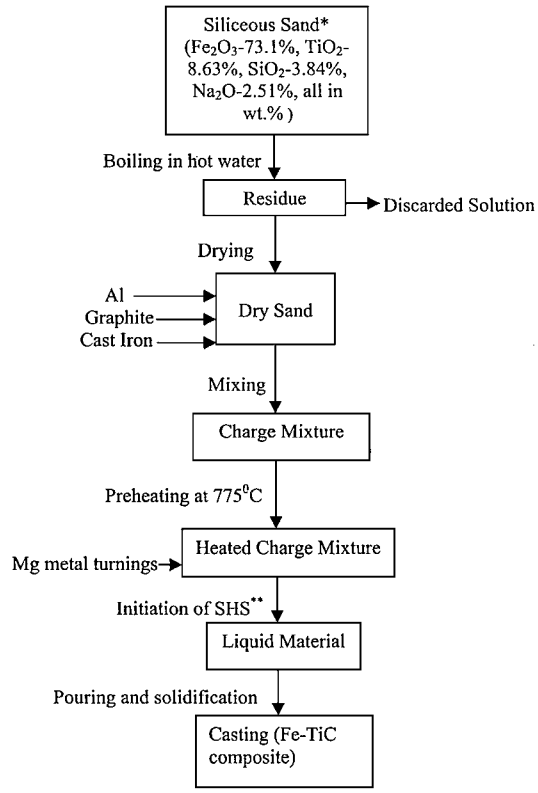

*Siliceous sand is a waste material from aluminium extraction plant.
**SHS means self-propagating high temperature synthesis.

Figure 13 Flow chart depicting the synthesis of Fe-TiC composite from siliceous sand [44].

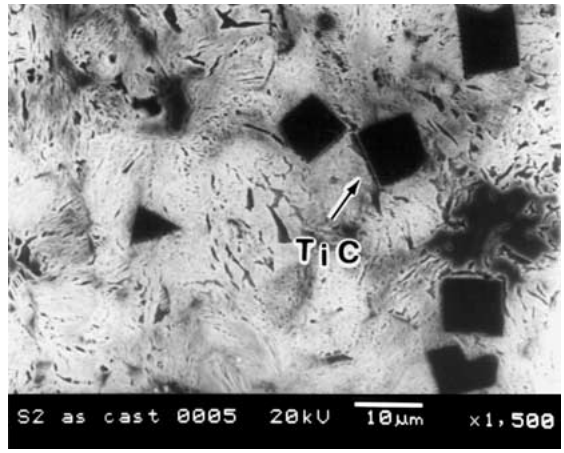

Figure 14 SEM micrograph showing distribution of TiC particles in pearlitic type matrix [44].

The main advantage of producing Fe-based composite via aluminothermic reduction is the simplicity of the method by which the composite can be produced. The heat evolved during aluminothermic reduction will melt the charge. Therefore, no expensive experimental set up but only some cheap raw materials are needed to synthesize the composite. As a result, even a small-scale foundry can produce Fe-based composite with improvement in properties over conventional steel/cast iron castings.

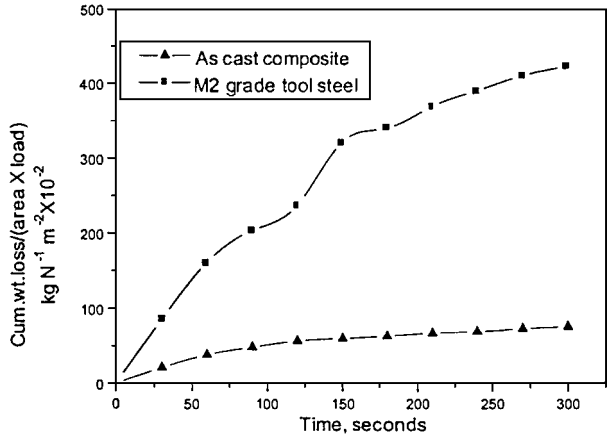

Figure 15 Comparison of wear behavior between as cast composite and tool steel [44].

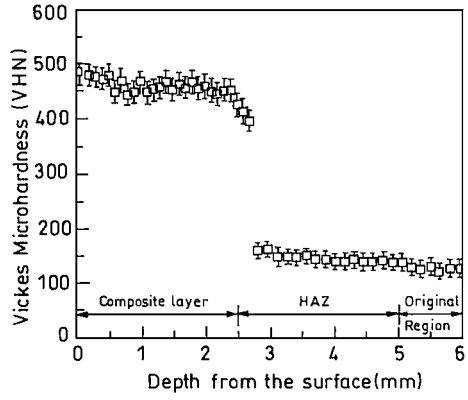

Figure 17 Vickers hardness vs. depth from the irradiated surface of the TiC-reinforced surface composite [47].

2.6. TiC reinforced ferrous surface composites fabricated by electron beam radiation/laser surface melting/plasma spray synthesis

In the recent years attempt had been made to achieve surface hardening or surface alloying by direct irradiation with high-energy electron beam [45, 46]. Soon-Ju Kwon *et al*. [47] tried a very simple method where TiC powder having a purity of 99% and size of 2–5 μm was mixed with 10 wt% flux (MgO & CaO at 1:1 ratio) and homogeneously deposited on a plain carbon steel (Fe-0.1C-0.24Si-0.56Mn-0.16Cu-0.08Ni-0.06Cr-0.02Al-0.01P–0.03S) substrate. It was then irradiated with a high-energy electron beam under conditions of 1.4 MeV beam energy, 1.2 cm beam diameter, 1 cm/s beam traveling speed. The flux was used to protect melted TiC powder from air and to control the composition. A schematic of the process is shown in Fig. 16. The material produced in this way had a top layer consisting of Fe-TiC composite with a hardness of 400–490 VHN followed by a coarse grained heat affected zone with a hardness of 170 VHN, a fine grained heat affected zone with a hardness of 150 VHN and then the unaltered matrix with a hardness of 130 VHN (Fig. 17). Thus, by this method the hardness of the surface had been increased by three to four times over the unaltered surface by impregnating the bainitic matrix with radially grown dendrites of TiC, particles, and fine needle shaped eutectic TiC particles.

TiC hardened steel surfaces had also been produced by laser surface melting [48, 49, 50]. Ayers and Tucker [49] had processed TiC hardened steel surfaces by laser surface melting. A CO_2 laser was used to melt a shallow pool on the surface of a 304 stainless steel piece. The carbide powder carried by a stream of helium was blown into the melt from a nozzle positioned about 1 cm away. The TiC particles were injected in this way, otherwise they would float on the top owing to the density difference between TiC and stainless steel. Microhardness measurements were taken from the matrix and macrohardness measurements were taken from the composite material. The hardness of the matrix when injected with +140, −70 mesh TiC particle varied between 205 and 253 HV with an average value of 219 HV and the hardness of the matrix when injected with +325, −230 mesh TiC particle varied between 242–272 HV. The increased microhardness of the austenetic matrix from 152 HV to values of about 200–270 HV was due to the partial dissolution of the carbide particles. It was also concluded that the finer the carbide particles, the more was the dissolution and thereby the greater was the hardness of the matrix. The macrohardness of the surface composite was about 57.6 HRC. However, surface composites produced by this method were never defect free. The injected carbide particles frequently got cracked due to the thermal stress imposed on them by the matrix during cooling. However, Ceri *et al*. [51] and Ariely *et al*. [52] claimed that the carbide reinforced surface composite produced by a laser injection technique was defect free.

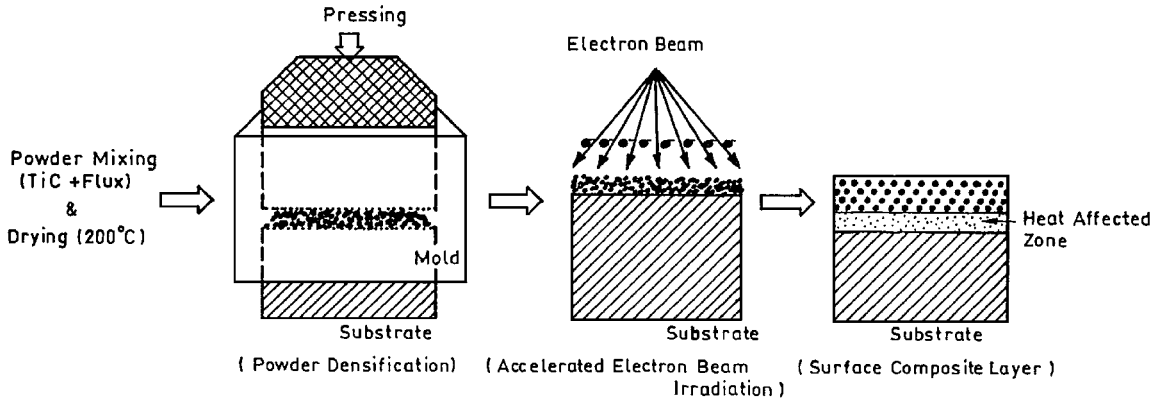

Figure 16 Schematic diagram showing the fabrication procedures of the TiC-reinforced ferrous surface composite [47].

Fasasi *et al*. [53] had also produced Fe-TiC surface composite by laser surface melting. A mixture of submicron size TiC particles and polyethylene glycol (PEG) was brought into a pasty state by heating the mixture to the melting point of the polymer, which is 70°C. The paste was then deposited on a Fe block and left to dry. The Nd^{3+} YAG laser was then passed over the surface. The composite structure at the surface was martensitic impregnated with TiC particles and was free of cracks even after rapid solidification and this could lead to the improvement of wear properties of martensitic steel. Surface hardness as high as 1400 kg mm^{-2} could be achieved by this method.

3. Concluding remarks

The present article provides an overview of the various synthesis routes of Fe-TiC composites, which have been evolving over the years. Although most of the commercially available Fe-TiC composites are processed by a powder metallurgy route, materials designers are in constant search for noble and also economical synthesis route, which may give us products with properties superior to the existing ones. As a result, various other routes such as a normal melting and casting route, a carbothermic reduction route, etc. have been tried by many research groups to produce *in situ* Fe-TiC composites with a uniform dispersion of TiC reinforcement. Combustion synthesis has also been used to synthesize TiC-Fe composite rather than Fe-TiC composite. The main purpose of synthesizing Fe-TiC composite is to use it as a wear resistant material. It has been found that a phenomenal improvement in wear resistance occurs owing to the incorporation of TiC particles in an Fe matrix. It has also been found that the wear resistance of the material increases with the decrease in particle size and also with the increase in carbide volume fraction. In an attempt to refine the TiC particle size, rapid solidification has come into the picture and subsequently people have tried to produce the submicronic TiC particle by techniques of laser surface melting, plasma spray synthesis, ion beam radiation, etc. The authors of the present article have produced Fe-TiC composite with an attractive wear resistance property by aluminothermic reduction of a discarded by product. This route of synthesis is not only economical but also capable of producing TiC particles whose size is somewhere between the size of TiC particle produced by conventional melting and laser surface melting, plasma spray synthesis, or ion beam radiation.

References

1. E. PAGOUNIS, M. TALVITIE and V. K. LINDROOS, *Metall. Mater. Trans. A* **27A** (1996) 4171.
2. *Idem*., *ibid.* **27A** (1996) 4183.
3. T. Z. KATTAMIS and T. SUGANUMA, *Mat. Sci. and Technol*. A **128** (1990) 241.
4. J. M. PANCHAL, T. VELA and T. RABISSCH, in "Fabrication of Particulate Reinforced Composites" (ASM International, Materials Park, OH, 1990) p. 245.
5. J. KUEBARSEPP, PhD thesis, Tallin Technical University, Tallin, 1992, p. 8.
6. E. PAGOUNIS, M. TALVITIE and V. K. LINDROOS, *Powder Metall*. **40** (1997) 55.
7. Y. B. LIU, S. C. LIM, L. LU and M. O. LAL, in "Metal Matrix Composites" (Woodhead Publishing, Madrid, 1993) p. 770.
8. B. S. TERRY and O. S. CHINYMAKOBVU, *J. Mater. Sci. Lett.* **10** (1991) 628.
9. Technical literature from "Chromalloy," Metal Tectonics Company Bulletin 54, Sinter Cast Division, Western Highway, West Nyack, New York 10994.
10. H. SEILSTORFER and G. MOSER, *Metall*. **10** (1980) 925.
11. J. D. BOLTON and A. J. GANT, *Powder Metall*. **40** (1997) 143.
12. R. K. GALGALI, PhD thesis, Indian Institute of Technology, Kharagpur, 1995.
13. B. S. TERRY and O. S. CHINYMAKOBVU, *Mat. Sci. and Technol*. **8** (1992) 399.
14. C. RAGHUNATH, M. S. BHAT and P. K. ROHATGI, *Scripta Metall*. **32** (1995) 577.
15. S. SKOLIANOS, T. Z. KATTAMIS, M. CHEN and B. V. CHAMBERS, *Mat. Sci. and Technol.* A **183** (1994) 195.
16. A. A. POPOV and M. M. GASSIK, *Scripta Materialia* **35** (1996) 629.
17. Z. LIU and H. FREDRIKSSON, *Metall. Mater. Trans. A* **28A** (1997) 471.
18. *Idem*., *ibid*. **28A** (1997) 707.
19. D. R. GASKELL, in "Introduction to Metallurgical Thermodynamics" (McGraw Hill, New York, 1971).
20. O. KUBASCHEWSKI, C. B. ALCOCK and P. J. SPENCER, in "Materials Thermochemistry" (Pergamon Press, Oxford, 1993).
21. B. S. TERRY and O. S. CHINYAMAKOBVU, *Mat. Sci. and Technol*. **7** (1991) 842.
22. Y. CHEN, *Scripta Materialia* **36** (1997) 989.
23. J. B. HOLT and Z. A. MUNIR, *J. Mater. Sci*. **21** (1986) 251.
24. J. J. MOORE and H. J. FENG, *Prog. in Mat. Sci*. **39** (1995) 243.
25. M. J. CAPALDI, A. SAIDI and J. V. WOOD, *ISIJ International* **37** (1997) 188.
26. N. SATO and Z. A. MUNIR, in Proceedings of the Symposium on High Temperature Materials V, edited by W. B. Johnson and R. A. Rapp (Electrochemical Society, Pennington, NJ, 1996) Vol. 9–18, p. 99.
27. K. S. VECCHIO, J. C. LASALVIA and M. A. MEYERS, *Met. Trans. A* **23A** (1992) 87.
28. A. HERNANDEZ-GUERRERO, Z. HUQUE and A. M. KANUARY, *Combust. Sci. and Tech.* **81** (1992) 115.
29. O. YAMADA, Y. MIYAMOTO and M. KOIZUMI, *J. Amer. Ceram. Soc*. **70** (1987) 206.
30. Y. CHOI and S.-W. RHEE, *J. Mater. Sci*. **28** (1993) 6669.
31. L. J. KECSKES, T. KOTTKE and A. NIILER, *J. Amer. Ceram Soc*. **73**(5) (1990) 1274.
32. H. A. GREBE, A. ADVANI, N. N. THADHANI and T. KOTTKE, *Met. Trans A* **23A** (1992) 2365.
33. S. D. DUNMEAD, D. W. READEY and C. E. SEMLER, *J. Amer. Ceram. Soc*. **72**(12) (1989) 2318.
34. D. C. HALVERSION, K. H. EWALD and J. A. MUNIR, *J. Mater. Sci*. **28** (1993) 4583.
35. E. ZHANG, S. ZENG, B. YANG, Q. LI and M. MA, *Met. Trans. A* **36A** (1999) 1147.
36. *Idem*., *ibid*. **36A** (1999) 1153.
37. Z. A. MUNIR and W. LAI, *Combust. Sci. & Tech*. **88** (1992) 201.
38. S. C. DEEVI, *J. Mater. Sci*. **26** (1991) 2662.
39. A. SAIDI, A. CHRYSANTHOU, J. V. WOOD and J. L. F. KELLIE, *ibid.* **29** (1994) 4993.
40. Y. CHOI and S.-W. RHEE, *J. Mater Res*. **8** (1993) 3202.
41. Q. FAN, H. CHAI and Z. JIN, *J. Mat. Process. Technol*. **96** (1999) 102.
42. J. D. VEROHOEVEN, in "Fundamentals of Physical Metallurgy" (Wiley, New York, 1975) p. 153.
43. L. L. WANG, Z. A. MUNIR and Y. M. MAXIMOV, *J. Mater. Sci.* **28** (1993) 3693.
44. T. K. BANDYOPADHYAY and K. DAS (unpublished research).
45. A. F. BAISMAN, S. B. VASSERMAN, M. G. GOLKOVSKII, V. D. KEDO and R. A. SALLIMOV, About Surface hardening by Concentrated Electron Beam at atmosphere, Preprint No. 88-73, Budker Institute of Nuclear Physics, Novosibrsk, Russia, 1988.

46. D. SUH, S. LEE, S.-J. KWON and Y. M. KOO, *Metall. Trans. A* **28A** (1997) 1.
47. S.-J. KWON, S.-H. CHO and S. LEE, *Scripta Materialia* **40** (1999) 235.
48. J. D. AYERS and R. J. SCHAEFER, in "Laser Application in Material Processing" (Society of Photo-Optical Instrumentation Engineers, Bellingham, Washington, 1979) p. 57.
49. J. D. AYERS, T. R. TUCKER and R. J. SCHAEFER, in Proceedings of the Rapid Solidification Processing Principles and Technologies, Reston, Virginia, March 1980, edited by M. Cohen, B. Kear and R. Mehrabian (Claiton's Publishing Division, Baton Rouge, Louisiana).
50. J. D. AYERS and T. R. TUCKER, *Thin Solid Films* **73** (1980) 201.
51. W. CERI, R. MARTINELLA, G. P. MOR, P. BIANCHI and D. D. ANGELO, *Surf. Coat. Technol.* **49** (1991) 40.
52. S. ARIELY, J. SHEN, M. BAMBERGER, F. D. DANSIGH and H. HUGEL, *ibid.* **45** (1991) 403.
53. A. Y. FASASI, M. PONS, C. TASSIN and A. GALERIE, *J. Mater. Sci.* **29** (1994) 5121.

Received 25 October 2001
and accepted 1 April 2002